Deep-Sea Research II 58 (2011) 2509–2523

Contents lists available at ScienceDirect

Deep-Sea Research II

journal homepage: www.elsevier.com/locate/dsr2

Warming of deep and abyssal water masses along the Greenwich meridian on decadal time scales: The Weddell gyre as a heat buffer

E. Fahrbach *, M. Hoppema, G. Rohardt, O. Boebel, O. Klatt, A. Wisotzki

Stiftung Alfred-Wegener-Institut für Polar- und Meeresforschung in der Helmholtz-Gemeinschaft, Fachbereich Klimawissenschaften, Sektion Messende Ozeanographie, Postfach 120161, D-27515 Bremerhaven, Germany

ARTICLE INFO

Available online 25 June 2011

Keywords:
Southern Ocean
Weddell Sea
Water masses
Decadal variability
Polarstern

ABSTRACT

The Southern Ocean renders a significant contribution to the global overturning system through the formation of deep and bottom waters. The Weddell Sea is one of the most prominent regions in this respect. Data obtained between 1984 and 2008 from eight repeat hydrographic sections, moored instruments and profiling floats in the Weddell gyre on the Greenwich meridian – almost all of them collected with RV *Polarstern* – were used to identify variations in the Weddell system. Fluctuations in the water mass properties were detected in the Warm Deep Water, with a temperature maximum in the 1990s and a minimum in 2005, but also significant variations occurred in the Weddell Sea Deep and Bottom Waters, whereas the Warm Deep Water is dominated by decadal variations; the average temperature and salinity of the whole water column is subject to a positive trend over 24 years. The variations of the water mass properties are induced by variations of the inflow of Circumpolar Deep Water at the boundary. Due to asymmetric wind forcing at the northern and the southern limb of the gyre, variable in- and outflows occur at the open boundaries. Internal processes redistribute heat and salt in the gyre resulting in a long-term increase of the temperature and salinity in the whole water column. The transfer of heat to deeper layers assigns to the Weddell gyre the role of a buffer, with potential impact on the global climate.

1. Introduction

The overturning circulation of the world oceans is a powerful process to store heat and gases in the deep ocean and as such an important component of the climate system. As part of this, the Southern Ocean is pivotal, connecting all major oceans basins (e.g., Rintoul et al., 2001; Schmitz, 1996). In the Southern Ocean, shoaling Circumpolar Deep Water (CDW) feeds into a shallow meridional overturning cell leading to the formation of intermediate waters, and a deep cell transforming Circumpolar Deep Water and forming Antarctic Bottom Water (AABW). A major contribution to the deep and bottom water formation is made by the Atlantic sector, i.e., the Weddell Sea (Carmack, 1977; Orsi et al., 1999; Rintoul, 1998). This water mass transformation is controlled by the transport of source waters into the Weddell Sea, processes within the Weddell Sea and the transport of modified water out of it (Foster et al., 1987; Gill, 1973; Mosby, 1934). In the Weddell Sea, CDW enters from the east and the north and circulates as Warm Deep Water (WDW) in intermediate depths within the large-scale cyclonic gyre (Fig. 1). This flow regime is confirmed on the basis of data from vertically profiling floats deployed on the Greenwich meridian and in the Weddell Sea (Fig. 2) and moorings in the northern and southern limb of the gyre (Fig. 3). WDW is the main source water of the other major water masses of the Weddell gyre, namely the Weddell Sea Bottom Water (WSBW) and Weddell Sea Deep Water (WSDW).

Observations have demonstrated that the global ocean has been warming (Gouretski and Koltermann, 2007; Levitus et al., 2005). In the Southern Ocean a warming trend over several decades is identified in the upper parts of the Circumpolar Deep Water (Böning et al., 2008; Gille, 2008; Sprintall, 2008). There is evidence that the Antarctic Bottom Water is subject to change, albeit becoming colder and fresher (Aoki et al., 2005; Johnson et al., 2008; Rintoul, 2007) in the Indian and Pacific sectors of the Southern Ocean. Warming of AABW was observed in the Atlantic Ocean in the Vema Channel (Zenk and Morozov, 2007), near the equator (Andrié et al., 2003), and basin wide (Purkey and Johnson, 2010). We explore the processes that determine the way in which global warming affects water mass formation in the Weddell Sea, the latter being a major source of AABW.

It has been long known that WDW shows significant variations from year to year (e.g., Gordon, 1982). With long term observations based on repeat hydrographic data, decadal variations may be examined. Warming and a salinity increase of the WDW

* Corresponding author. Tel.: +49 471 4831 1820; fax: +49 471 4831 1797.
E-mail address: Eberhard.Fahrbach@awi.de (E. Fahrbach).

0967-0645/$ - see front matter © 2011 Published by Elsevier Ltd.
doi:10.1016/j.dsr2.2011.06.007

observed during the 1990s were followed by cooling during the 2000s (Fahrbach et al., 2004; Robertson et al., 2002). The variations are most likely due to changes in the inflow from the circumpolar water belt, which are induced by changes in atmospheric forcing conditions. Various modes of climate variability in the Southern Ocean are known, of which the Southern Annular Mode (Hall and Visbeck, 2002; Thompson and Solomon, 2002) is the most important, and these may affect the Weddell Sea. Kerr et al. (2009) indeed suggested a correlation between the Southern Annular Mode and the Weddell Sea Bottom Water. Sallée et al. (2010) show that a recent trend in the SAM leads to a more southern path of the westerly winds and changes in mixed layer depths. Whereas the variations of properties of the Weddell Sea Deep Water have long time remained within the uncertainty of our observations, the observed changes in the Weddell Sea Bottom Water were found to be significant (Fahrbach et al., 2004). Since the WDW is one of the source components of bottom water, the variations of the two water masses are possibly related through the formation process; using our unique repeat section time series we explore also other explanations.

We use the term Weddell gyre for the circulation system reaching from the Weddell Sea up to 30°E into the Enderby basin in the Indian sector and the term Weddell system for the combination of advective and transformation processes which in the Weddell gyre acts to produce from the inflowing source water the deep water masses contributing to the global overturning. In this study we show that even when the properties of WDW in the Weddell gyre are subject to decadal fluctuation, the excess of heat and salt transported during such events is stored in the deep and abyssal water masses inducing an increase of temperature and salinity. It follows that the processes in the Weddell system, despite of producing cold and low salinity Weddell Sea Bottom Water, transfer heat and salt from the CDW directly into the Weddell Sea Deep Water without necessarily affecting the bottom water production.

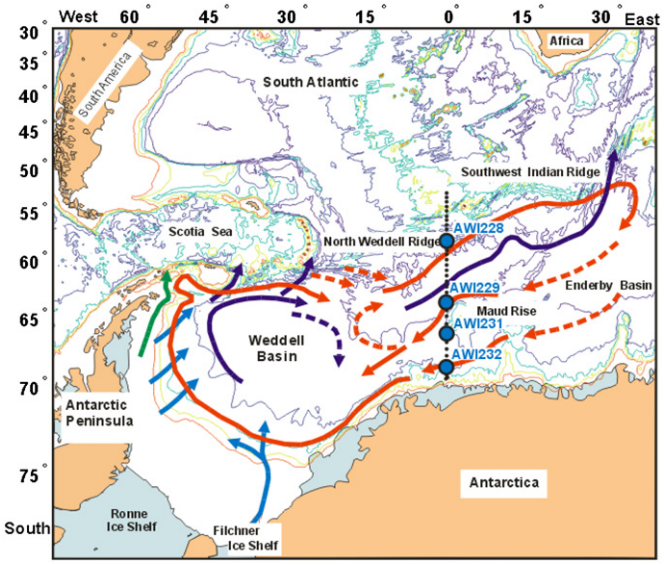

Fig. 1. Map of the Atlantic sector of the Southern Ocean including the generalized circulation of the Weddell gyre, the location of the section at the Greenwich meridian and of the moorings AWI 228, AWI 229, AWI 231 and AWI 232. Red arrows indicate circulation of Circumpolar (Warm) Deep Water, and light blue arrows sinking water masses along the continental slope. Dark blue arrows depict deep and bottom water circulation and water masses leaving the basin. The green arrow indicates shelf water leaving the western Weddell Sea. Dashed arrows indicate either transient currents or eddy exchanges.(For interpretation of the references to color in this figure legend, the reader is referred to the web version of this article.)

2. The data

Almost all data were collected during cruises with the ice breaker RV *Polarstern* between 1992 and 2008 (except for the AJAX cruise in 1984). This warrants a high consistency of the data set. The data set obtained in 2008 (Fahrbach and De Baar, 2010) was part of an International Polar Year project called Climate of Antarctica and the Southern Ocean (CASO; http://classic.ipy.org/development/eoi/proposal-details.php?id=132). Some sections were occupied as part of the WOCE Repeat Sections Program (Siedler et al., 2001). Later repeats along the Greenwich meridian are a contribution to CLIVAR (http://www.clivar.org/organization/southern/southern.php). All data are available at international data centers and have so far appeared in several publications (e.g., Fahrbach et al., 1995, 2004). A data collection highlighting 25 years of *Polarstern* hydrographic data, and including all but the most recent data used here, was released (Fahrbach et al., 2007). *Polarstern* plies this region of the Southern Ocean, in particular two different sections: one along the Greenwich meridian from the southern part of the Antarctic Circumpolar Current to the Antarctic continent, thus completely crossing the Weddell gyre at this longitude, and a second along a line connecting Kapp Norvegia and Joinville Island at the tip of the Antarctic Peninsula (WOCE section

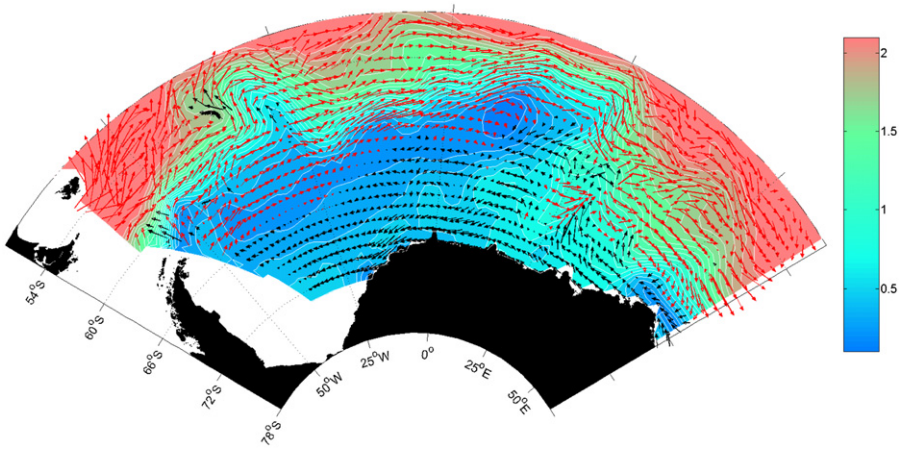

Fig. 2. The Weddell gyre flow and in-situ temperature in 800 m depth derived from the data of 206 ice-compatible vertically profiling floats (Klatt et al., 2007) between 1999 and 2010. Red arrows indicate eastward currents, and black arrows westward currents.(For interpretation of the references to color in this figure legend, the reader is referred to the web version of this article.)

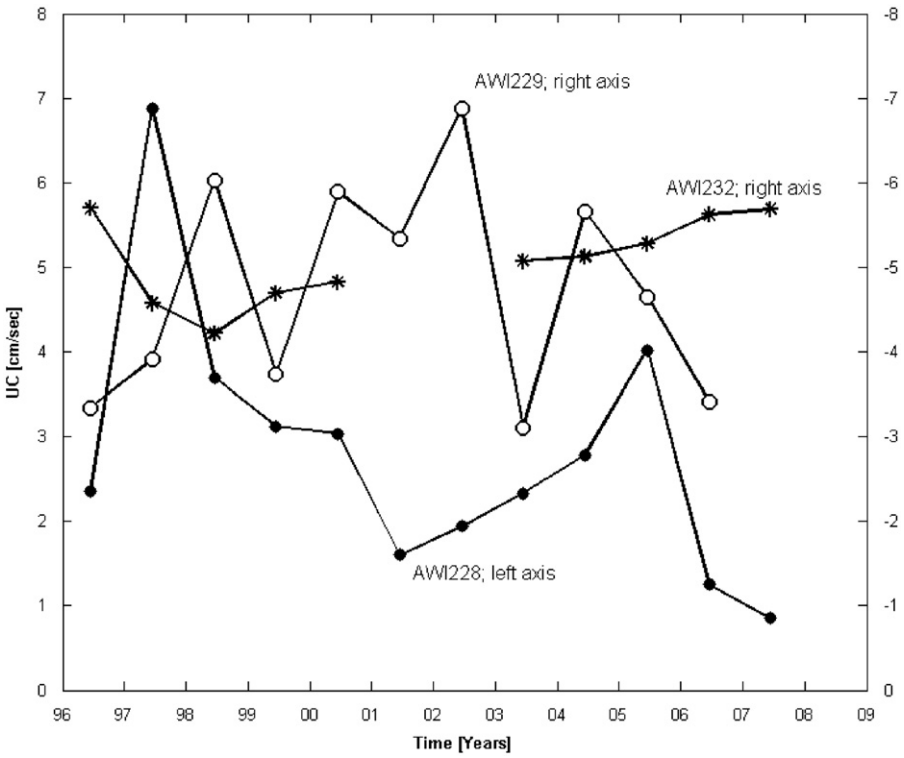

Fig. 3. Annual averages of the zonal component of current meter records in the northern limb of the Weddell gyre in 500 m depth (mooring AWI 228), in the southern limb of the gyre north of Maud Rise in 700 m depth (mooring AWI 229) and in the southern limb south of Maud Rise in 700 m depth (mooring AWI 232). The location of the moorings is indicated in Fig. 1.

SR4) thus pinching off the Weddell Sea to the southwest. Here we focus on the data from the Greenwich meridian section. Generally the stations follow the lines within a few km, but in some cases (AJAX) the distances from the lines are somewhat larger.

Data sets from the Greenwich meridian (southern part of WOCE section A12) include

AJAX (leg 2)	16–29 January 1984
ANT-X/4:	5–19 June 1992
ANT-XIII/4	12–23 April 1996
ANT-XV/4	29 April–16 May 1998
ANT-XVIII/3	20 December 2000–2 January 2001
ANT-XX/2	30 November–19 December 2002
ANT-XXII/3	31 January–09 February 2005
ANT-XXIV/3	19 February–12 March 2008

All temperature and salinity data were collected with a CTD instrument (conductivity, temperature, and depth) fixed to a 24-place rosette sampler with 12 l bottles. Details can be found in Fahrbach et al. (2004, 2007) and Fahrbach and De Baar (2010). Since 2000 a Seabird SBE 911plus CTD has been in use. Salinities are reported on the Practical Salinity Scale (PSS78). Data of all cruises are accurate to at least 0.003 °C in temperature, 2 db in pressure and 0.003 in salinity. The high consistency of the properties observed in the relatively stable Weddell Sea Deep Water suggests that the accuracy is higher, notably 0.001 °C in temperature and 0.001 in salinity (Fahrbach et al., 2004). Using a large number of independent measurements, the ultimate accuracy is determined by the calibration procedure. As to temperature, the accuracy left after calibration by the manufacturer or the Scripps Institution of Oceanography is 0.001 °C. The accuracy of the salinity has always been set by calibration with IAPSO standard seawater, which is better than 0.001 (Culkin and Ridout, 1998). For the AJAX data collected with RV *Knorr* refer to Chipman et al. (1986) and Whitworth and Nowlin (1987).

Moorings were maintained at the Greenwich meridian between 69.5°S and 57°S from 1996 to 2008 and they carried current meters, temperature sensors and upward looking sonars (Fahrbach and De Baar, 2010; Klatt et al., 2005). Here we present data from moorings AWI 228, AWI 229, AWI 231 and AWI 232 (Fig. 1). The number of instruments and the time span in which they were active differ between moorings. We present data from Seabird Microcats and Aanderaa thermistor strings TK250. The thermistors were calibrated by Aanderaa before and after the mooring period. Since the accuracy of the CTD temperature sensor is much higher than that of the moored instruments, the records of the moored instruments were corrected with a constant offset to match the CTD profile at the time of deployment of the instruments. The data were essentially processed as described previously in Fahrbach et al. (1994).

Depending of the vertical current profile and mooring configuration, the motions of the moorings were generally significant, resulting in noticeable vertical displacements of the sensors. The strongest displacements occurred at AWI 229 by up to 300 m. Deviations of this scale require corrections of the measured temperature and salinity. Since not all instruments were equipped with pressure sensors, the displacement of instruments without pressure sensor had to be determined. According to the mooring configuration, the motion can be approximated either by a solid rod or a rope like the string of a kite. With the software package "MOORDESIGN" (Dewey, 1999, 2009), it was determined which of the two models would fit the observed mooring displacement closer by applying cosine functions or second-order polynomial fits. On the basis of the selected model, the depths of the instruments without pressure sensor were estimated.

Since the pressure records of Aanderaa current meters have a lower resolution than those of Seabird Microcat/Seacat, the

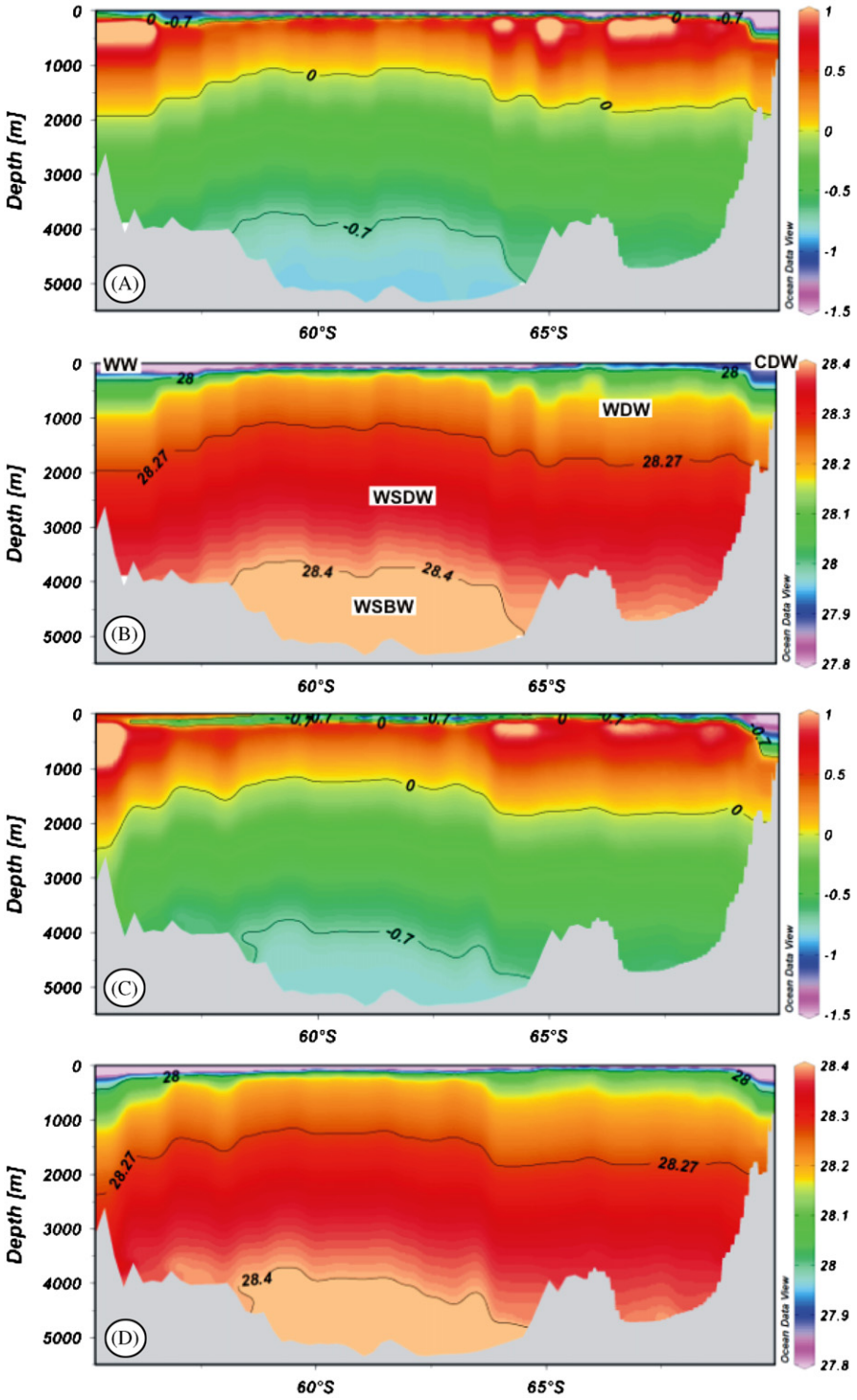

Fig. 4. Vertical sections of potential temperature (A and C) and neutral density (B and D) along the Greenwich meridian from the Southwest Indian Ridge (left) to the Antarctic continent (right) as measured during *Polarstern* cruises ANT-X/4 in 1992 (A and B) and ANT-XXIV/3 in 2008 (C and D). The main water masses are the Circumpolar Deep Water (CDW), the Warm Deep Water (WDW), the Weddell Sea Deep Water (WSDW) and the Weddell Sea Bottom Water (WSBW). The reduction of the areal extent of WSBW (< -0.7 °C) by 25% is clearly visible. Contour plots created with ODV (Schlitzer, 2010).

former were only used in the absence of a Seabird instrument with pressure sensor. Right after deployment, most pressure records showed an exponential adjustment to the real instrument depth, which had to be corrected. The computed time series of temperature and salinity were checked within the mooring and the Θ/S-diagrams of the Microcats were adjusted to those of CTD data obtained during deployment- and recovery cruises.

Since 1999, AWI deployed more than 130 Argo floats within the Weddell gyre. Delayed mode quality control was applied according to Argo standard (Owens and Wong, 2009), comparing float data to high quality reference CTD data (climatology). These comparisons were made on deep isotherms and assumed that the temperature sensor of the float is stable and that salinity on deep isotherms was steady and uniform. The accuracy of the float data

is better than 0.01 °C in temperature and 0.01 in salinity (Argo standard).

3. Results

3.1. The mean water mass properties

The section of potential temperature along the Greenwich meridian obtained during cruise ANT-XXIV/3 in 2008 and the first section occupied by *Polarstern* during cruise ANT-X/4 in 1992 serve as a background for the hydrographic situation (Fig. 4). Detailed accounts on the hydrography of the region have been published by Deacon (1979), Whitworth and Nowlin (1987), Orsi et al. (1993), Schröder and Fahrbach (1999) and Fahrbach et al. (2004). The northern boundary of the Weddell gyre at this longitude occurs at about 56°S (Klatt et al., 2005). The position of the front is topographically controlled by the North Weddell and the South Indian Ridge, but it is not immovable due to variability of and interactions with the Antarctic Circumpolar Current (ACC) to the north and the Weddell gyre flow to the south. It may be placed at the location where the core of warm water from the ACC meets the much colder subsurface water from the Weddell gyre, i.e., where the lateral temperature gradients are the highest and the density gradients point to high currents. Although relatively warm Circumpolar Deep Water from the ACC may intrude into the gyre at its northern boundary (Fahrbach et al., 2004; Klatt et al., 2005), the major part of the warm water is supplied to the gyre near its eastern end (Bagriantsev et al., 1989; Deacon, 1979; Gouretski and Danilov, 1993; Schröder and Fahrbach, 1999). After entering the gyre, the CDW (then known as Warm Deep Water) joins the circulation as subsurface water in the southern limb of the gyre in 60–68°S, recognizable by a potential temperature maximum of 0.6–1.0 °C at 200–300 m depth. Note that the region of the potential temperature maximum is split at about 66°S due to the circulation–topography interactions induced by the seamount Maud Rise. In the northern limb (56–60°S) the WDW temperature is lower. This is caused by mixing with colder waters above and below on its course through the gyre. Accompanying the potential temperature maximum are salinity, nutrients and total CO_2 maxima, and an oxygen minimum. Due to the northward Ekman transport in the Antarctic Circumpolar Current and the northern limb of the Weddell gyre, surface water is generally not able to penetrate into the gyre from the north, but only in the south as part of the slope current and coastal current (e.g., Núñez-Riboni and Fahrbach, 2009). Apart from that, water with characteristics of Weddell Sea Deep Water (see below) enters the gyre from the east (Heywood et al., 1999) along the coast with its core at about 3500 m depth. This cannot be distinguished in temperature–salinity fields, but stands out as a CFC maximum (Hoppema et al., 2001; Meredith et al., 2000).

The lower boundary of the WDW is defined at 0 °C (Reid et al., 1977). All water masses colder than 0 °C must derive from local processes because such waters cannot originate from the ACC to the north. Underneath the WDW the WSDW occurs as the most voluminous water mass of the Weddell gyre. WSDW is separated from the Weddell Sea Bottom Water by the −0.7 °C isotherm (Carmack and Foster, 1975), which at the Greenwich meridian is only found north of Maud Rise (Fig. 4). WSBW is formed in the southern and western Weddell Sea through downward flow of dense shelf waters into the deep sea, on its way entraining deep water, and it is transported to the east within the northern limb of the gyre (Foldvik et al., 2004; Nicholls et al., 2009). At the bottom a temperature minimum is characteristic of WSBW. Although direct WSDW formation from surface water and WDW occurs (Fahrbach et al., 1995; Orsi et al., 1993; Schlosser et al., 1991; Weppernig et al., 1996), most WSDW is thought to be a large-scale mixing product of WDW and WSBW within the gyre (e.g., Foster and Carmack, 1976). The potential temperature of the WSDW monotonically changes between that of the WSBW and the WDW. Due to its large volume and the weak currents (Klatt et al., 2005) resulting in a relatively long residence time, WSDW is thought to be the most stable water mass of the region. Since WSDW occupies a depth range that allows it to escape across the ocean ridges to the north (Naveira Garabato et al., 2002a, 2002b), it is the major source of Antarctic Bottom Water.

Since the Weddell gyre is a cyclonic feature, upwelling of subsurface water into the surface layer occurs in the interior of the gyre, frequently denoted as the Antarctic Divergence (Deacon, 1979). On gyre scale this can be discerned by doming of the isotherms (Fig. 4), which reach their shallowest depth towards the center of the gyre (60–62°S). Also the surface layer is the shallowest in this area. Note that on the Greenwich meridian, the gyre is strongly asymmetric with a relatively narrow (order of 500 km) northern limb of eastward flow and a relatively broad southern part (order of 1500 km). This is related to the topographical conditions with the seamount Maud Rise at 66°S, and the wind fields with the southward transition from westerly to easterly winds at approximately 65°S.

3.2. Variations of the deep and bottom water masses

Significant variations of the WDW and CDW properties have been reported before (Fahrbach et al., 2004; Gille, 2002; Leach et al., 2011; Meredith et al., 2001; Robertson et al., 2002). The section data in the present study constitute an extension by 6 years of the data presented by Fahrbach et al. (2004). This data set is complemented with long-term mooring data from the Greenwich meridian and with float data and will allow a more comprehensive view of the variations and strengthening of conclusions. We calculated temperature and salinity time series using all section data at the Greenwich meridian from 1984 to 2008. Computing methods were similar to those described by Fahrbach et al. (2004). However, neutral density (Jackett and McDougall, 1997; McDougall and Jackett, 2004) surfaces were used as water mass boundaries guided by the assumption that properties of a layer defined by neutral density limits are more conservative than properties of a layer defined by potential temperature limits. It can be seen that differences between the temperature and the neutral density boundaries are barely visible (Fig. 4). For investigating the large-scale picture, cross-basin averages of potential temperature and salinity were computed in order to diminish the effect of small to meso-scale features on the detection of low period changes of water mass properties. This was done for three deep water masses: WDW, WSDW and WSBW as defined by the neutral density limits of 28.00, 28.27 and 28.40 kg/m^3, which correspond closely to the 0° and −0.7 °C potential temperature limits used before. The changes of the mean temperature of the respective water masses are related to the heat content by their layer thicknesses (Fahrbach et al., 2006; Smedsrud, 2005). To the north the calculations were limited to 56°S (as opposed to 55°S in Fahrbach et al., 2004), whereas to the south the continent constitutes a natural boundary. The northern limit was selected in order to reduce effects of comparably small displacements of the front between Weddell gyre and ACC. High inter-annual variability near the northern rim was reported by Martinson and Iannuzzi (2003). In order to investigate the influence of the cross-basin average we calculated averages from 56°S to 60°S (northern part of the gyre) and 60°S to 69.5°S (southern part of the gyre) separately. The results (not shown) for the northern limb are noisier than for the southern limb due to the large influence of relatively small variations of the Weddell

Front. This confirms our assumption that we would obtain a more representative measure of the low period variations of the gyre by averaging over large areas, i.e., a large number of stations.

To calculate the mean properties of the individual layers, the data set was gridded with a distance in the vertical of 1 m and 1 km in the horizontal. The uncertainty of the mean values is determined by the horizontal and vertical variations along each transect. With a correlation length of 50 km horizontally (i.e., more than the station distance) and 10 m vertically, we have about 5000–10,000 independent samples per water mass. On this basis the uncertainties for the mean potential temperatures and salinities were calculated from the standard deviation.

Within expectation, the most pronounced variations, in the order of 0.08 °C, were observed in the WDW (Fig. 5A), as previously reported by Fahrbach et al. (2004) and Smedsrud (2005). Due to basin-wide averaging, this range is significantly smaller than local variations (for the latter, see e.g., Leach et al., 2011). Inclusion of the AJAX data from 1984 suggests that the increase of potential temperature during the 1990s was preceded by and part of an earlier increase during the second half of the 1980s. Note that the shift to neutral density limits and the exclusion of the region between 55 and 56°S in this study has an influence on the value of the average potential temperature of the WDW, but not on the variations computed previously (compare with Fig. 5 of Fahrbach et al., 2004). From about 1998 to 2005, the mean potential temperature of the WDW decreased to a value near to the one of 1984. Data from 2008 show that the potential temperature decrease of the WDW has come to an end and a sharp increase has recommenced. The salinity of the WDW was on rise during the 1990s, reaching a maximum in 1998 and decreased to a minimum in 2005 after which it started to increase again (Fig. 5B). Thus, potential temperature and salinity of the WDW varied concomitantly.

Potential temperature of the WSBW decreased from 1984 to 1992 and increased again until 2002 staying almost constant from then on (Fig. 5E). A comparison of the sections occupied in 1992 and 2008 demonstrates a remarkable difference of the properties of the Weddell Sea Bottom Water. The area covered by WSBW decreased by 25% in 16 years (Fig. 4). In the long term from 1984 to 2008 the salinity decreased, with almost all of the decrease occurring between 1984 and 1992; a minimum was reached in 1998 (Fig. 5F).

There is an increase of the potential temperature of the WSDW from 1992 to 2005 and a decrease to 2008 (Fig. 5C). Also, the salinity of WSDW increased from 1992 to 2005, and decreased sharply since then (Fig. 5D). The highest potential temperature of

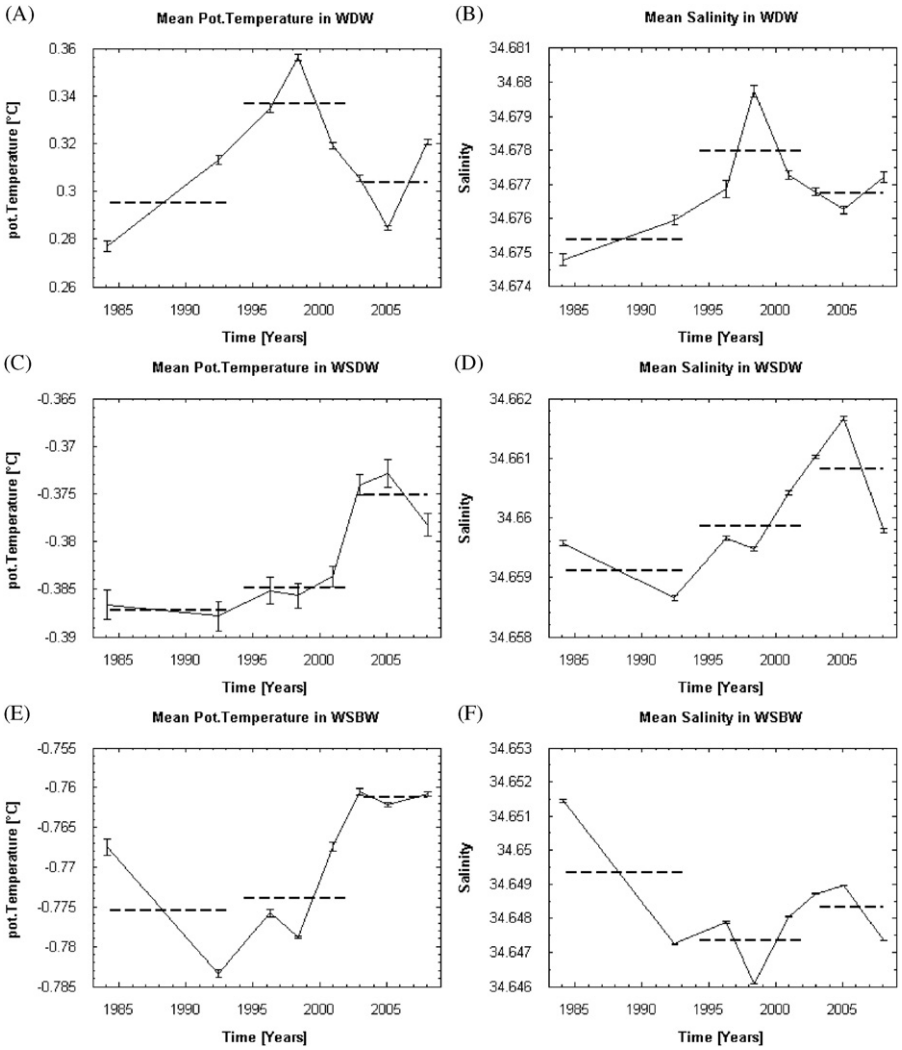

Fig. 5. Variations of the section mean potential temperature (°C) and salinity in the Weddell gyre from 1984 to 2008 observed on the Greenwich meridian between 56°S and the Antarctic continent. Water mass boundaries are defined by neutral density surfaces for Warm Deep Water (A and B), Weddell Sea Deep Water (C and D) and Weddell Sea Bottom Water (E and F). The error bars were calculated as the error of the mean value of independent samples. The time series are divided into three segments from 1984 to 1993, 1994 to 2002 and 2003 to 2008 for which the mean values are indicated by dashed line.

the WSDW was measured in 2005 simultaneously with the highest salinity.

Moored instruments were deployed and provide a quasi-continuous time series. We present a time series of temperature in the WDW (Fig. 6) obtained from an array of temperature sensors covering the period 1996–2008 at 64°S and 66.5°S along the Greenwich meridian (moorings AWI 229 and AWI 231, see Fig. 1). The potential temperature maximum of the WDW (200–300 m) is visible in this depth range. During periods when the thermocline reached deep enough it is recognizable by much lower temperatures at 150–200 m. The bottom end of the array was between 600 and 800 m, i.e., at about 0.3 °C and thus within the WDW. There are variations on seasonal, annual and multi-annual time scale as shown by Cisewski et al. (2011). The vertical extent of the WDW core decreased from 1996 to 2005 when the minimum temperature occurred and increased again after that. Due to the failure of the deep instruments from 2004 to 2005 this is less obvious in the record of mooring AWI 229 (Fig. 6 top). The temperature maximum is the highest at the beginning of the time series and the lowest in 2003/2004 at 64°S and 2005 at 66.5°S; generally, the temperature maximum was lower in the second half of the time series. The combined data sets suggest that the intensive annual or biannual fluctuations of the WDW temperature and layer thickness visible in the quasi-continuous records might affect the estimated intensity of the longer-term changes detected by means of repeat sections due to undersampling, but does not generate the decadal variations as a result of aliased higher-frequency signals (Fig. 6).

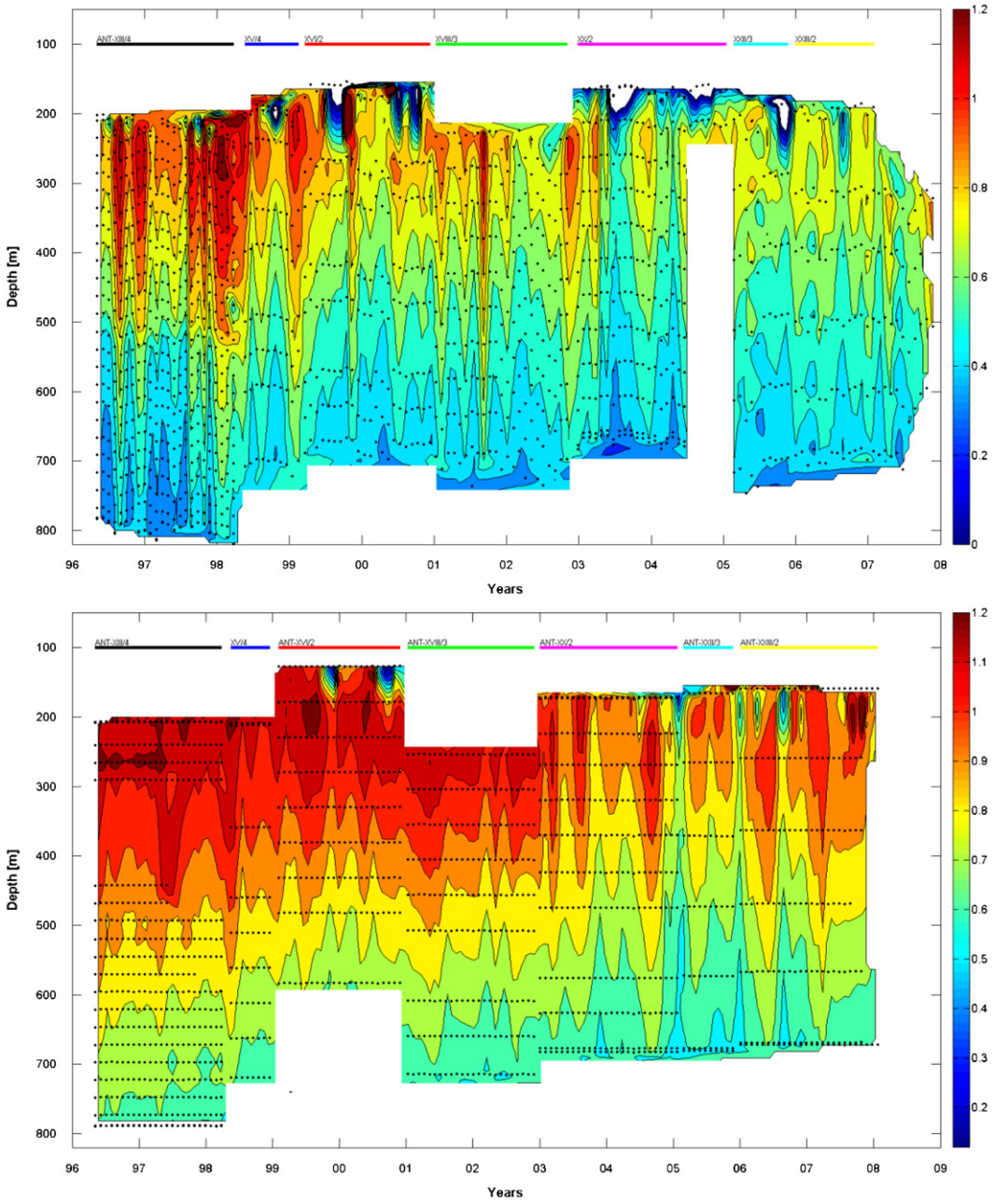

Fig. 6. Isopleth diagram of temperature in the Warm Deep Water from 1996 to 2008 at mooring AWI 229 located at the Greenwich meridian north of Maud Rise at 64°S (top) and AWI 231 south of Maud Rise at 66.5°S (bottom). For location see Fig. 1. The dots represent the depths of temperature sensors. Contours are drawn on the basis of monthly averages. The depth of the sensors was corrected for mooring motion. On top of the diagrams, the name of the cruise occurs during which the mooring was deployed. Mooring motion was much more intense at mooring AWI 229 than at mooring AWI 231.

4. Discussion

4.1. Potential causes of the variations

There are two processes that are potentially responsible for the variations of the deep water mass properties in the Weddell gyre:

- Variations of the inflow of CDW from the ACC into the Weddell gyre.
- Variation of the circulation within the gyre.

Variations in the inflow of CDW during the warming phase of the 1990s were discussed in Fahrbach et al. (2004), where especially instabilities of the Weddell gyre boundary were found to have an impact. Smedsrud (2005) emphasized ocean–ice–atmosphere interactions to be the cause of heat content changes in the Weddell gyre. We tried to compare the observed variations of the properties of the WDW to variations of the inflow properties, where we assume that variations of the volume of the water masses in the gyre are correlated to variations of the layer thickness (Fig. 7A). This assumption is valid, since we are discussing variations on the time scale of a decade or two which is long enough that a signal from the inflow is propagating through the gyre by advection and in consequence will not remain locally confined.

With increase in WDW temperature during the 1990s (Fig. 5A), the layer thickness increased from 1340 to 1390 m, while the subsequent cooling seems to roughly coincide with decrease of layer thickness, which reaches a minimum of 1340 m in 2001 (Fig. 7A). Note that this is earlier than the temperature minimum in 2005 (Fig. 5A). Both layer thickness and temperature increased from 2005 to 2008, where the former reached an absolute maximum of 1420 m. Fahrbach et al. (2004) explained the WDW warming during the 1990s by increased inflow due to instabilities of the boundary between Weddell gyre and ACC. This is consistent with a relatively large layer thickness in the 1990s (as an indicator of large volume). The warming during the 2000s is related to an increase of the layer thickness of 70 m again. A thicker WDW layer is likely to induce a shallower upper WDW limit (defined by the 0 °C isotherm or γ^n=28.0 kg/m^3), which in 2008 was relatively shallow with 118 m indeed (Fig. 7B). However, since the upper boundary of the WDW changed only by about 20 m the major volume increase of WDW (about 80 m) must have resulted from deepening of its lower boundary.

The WDW layer is ascending by upwelling in the interior of the cyclonic gyre and eroded at the top by entrainment into the Winter Water layer. At the bottom of the layer, mixing with the WSDW takes place. We expect that a transient inflow event is dissipated on a time scale of decades.

Since WDW is the main ingredient for WSBW and WSDW formation (Foster and Carmack, 1976), changes in these water masses are expected to be related. However, our data (Fig. 5) suggest that such relations are only valid over longer time scales. Actually, from 1984 to 1992 WSBW and WSDW temperatures and salinities decreased whereas the WDW was warming and increased in salinity. From 1998 onwards WDW was cooling and freshening whereas WSBW and WSDW were warming and their salinity increased (Fig. 5). This suggests that the variations in the WDW and WSBW/WSDW are either decoupled or subject to a time lag of the order of 5–10 years, which would be consistent with the typical time scale of the Weddell gyre circulation: WDW has to be advected from the Greenwich meridian into the WSBW/WSDW formation regions and the product has to return back to the Greenwich meridian. With a speed of 2–5 cm/s (Fig. 3) the distance of about 5800 km would take 3–8 years. This is consistent with the float data, which result in a time scale of about 5 years when combining the tracks in the southern and northern limb.

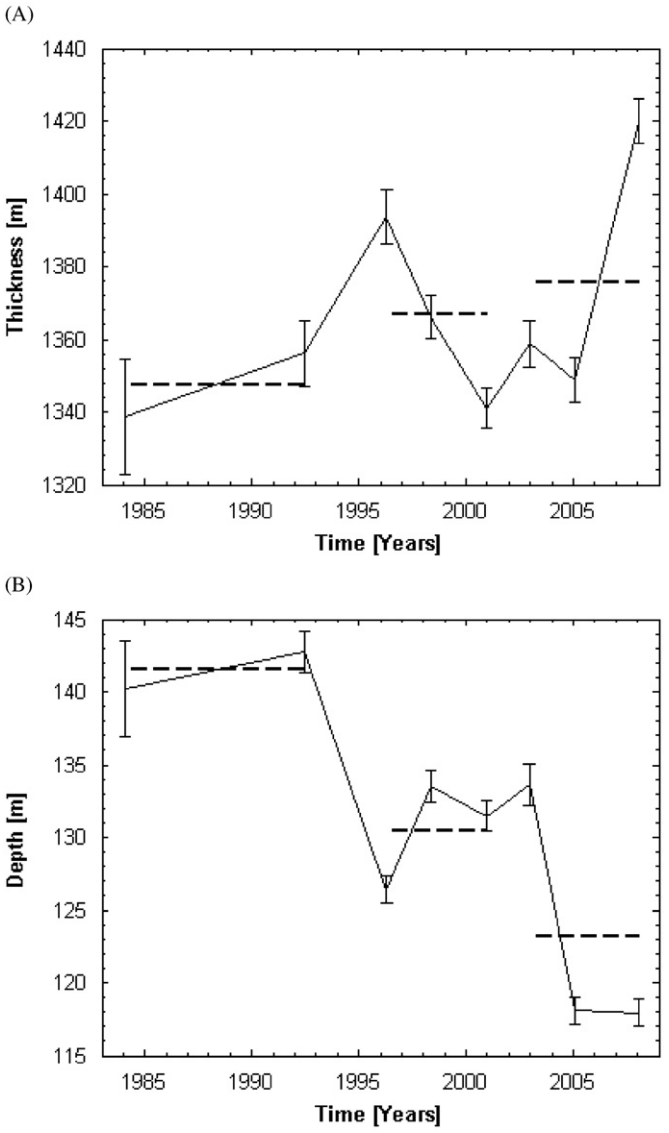

Fig. 7. Time series of properties of the Warm Deep Water as defined by neutral density over the section along the Greenwich meridian: (A) thickness of the WDW layer and (B) depth of upper limit of the WDW (at γ^n=28.0 kg/m^3). The time series are split into three segments from 1984 to 1993, 1994 to 2002 and 2003 to 2008 for which the mean values are indicated as dashed lines.

4.2. Variations in the Weddell gyre circulation

The cyclonic Weddell gyre circulation at the Greenwich meridian is evident in the tracks of the vertically profiling floats that display the eastward flow in the northern limb of the gyre and the westward flow in the south (Fig. 2) as a composite of data obtained from 1999 to 2010. This is consistent with the records from the current meter moorings between 1996 and 2008. The records indicate eastward current at mooring AWI 228 in the north and westward current at moorings AWI 299 and AWI 232 in the south (Fig. 3). The direct current measurements are consistent with the temperature and density fields displaying a doming of the isotherms (Fig. 4) and isopycnals. The doming of the isopycnals results in a trough of the geopotential anomaly (i.e., dynamic height) centered at 60°S (Fig. 8). Whilst the northern limb of the gyre clearly stands out by its geopotential anomaly

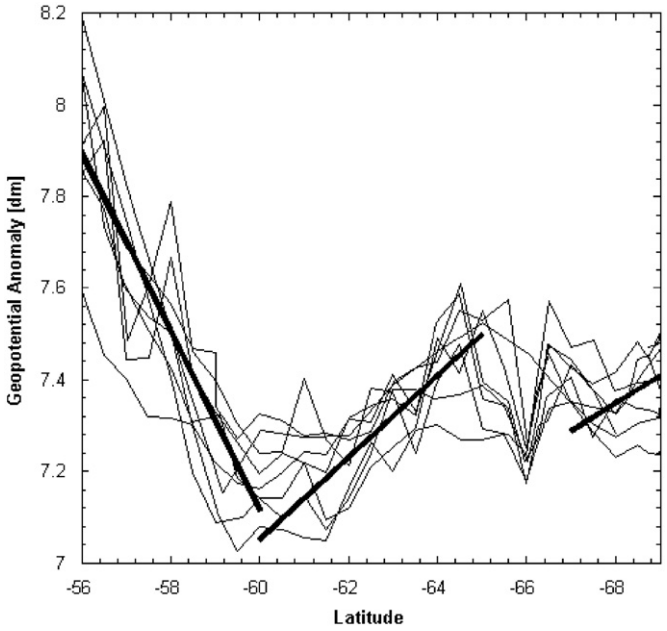

Fig. 8. Geopotential anomaly relative to 2000 db as a composite for all eight sections along the Greenwich meridian. The averages for the northern and the southern limbs of the Weddell gyre are displayed by thick lines. The southern limb is split into the area north and south of Maud Rise and the circulation around Maud Rise (about 66°S) is excluded from our considerations.

gradient, the southern limb flow is perturbed by Maud Rise (at about 66°S) where westward flow passes this seamount on its the northern side, while another part is deviated to the south (see also Leach et al., 2011) joining the Antarctic Slope Current. Topographical features like Maud Rise lead to locally trapped currents (e.g., Taylor column; Lindsay et al., 2008; Muench et al., 2001).

The hydrographic data cover the longest time period of our observations, namely from 1984 to 2008. The current meter records from 1996 to 2008 cover a shorter time period but are free of the uncertainty of aliasing. Still, since the currents are seriously affected by small scale structures of local topography, we consider the gradient of the geopotential anomaly a more suitable indicator to the large-scale circulation. However, we have to take into account that the barotropic component of the current might not be fully represented by a constant reference level of 2000 db.

The northern and southern slopes of the geopotential anomaly were fitted by straight lines for all sections to obtain time series of the intensity of the gyre flow. To take into account the influence of Maud Rise, the southern slope was split into the parts north and south (67–69.4°S) of the seamount (Fig. 8). The southernmost part of the gradient associated with the shelf front is not included, since it is not relevant for the transport of deep water masses. The resulting time series are displayed in Fig. 9A–C. Steep dynamic topography concurs with strong flow and a gentle slope with weak flow. The scales clearly indicate the more intense narrow eastward flow in the north (Fig. 9A) and the more diffuse westward flow in the south (Fig. 9B). The variability of the flow is characterized by a trend with a superimposed decadal fluctuation. In the north the trend dominates and in the south the decadal fluctuation.

In order to correlate variations in the flow intensity, water mass properties and potential driving forces, the uncertainty due to higher frequency variations needs to be reduced. To this end we averaged the data in three intervals: 1984–1993, 1994–2002 and 2003–2008. These time intervals were defined on the basis of the wind variations displayed in Fig. 9D–F. The averages of the flow of the northern limb display a decrease of eastward flow with a minimum in the middle period (Fig. 9A). In the southern limb north of Maud Rise, strong westward flow is followed by a period of weak flow with subsequent partial recovery (Fig. 9B). In the area south of Maud Rise the flow decreases and even reverses to eastward flow in the 1993–2003 period with a subsequent recovery as well. Due to the limited time duration, the current meter data can only confirm during the second part of the observation period from 1996 to 2008 the decreasing eastward current in the north (mooring AWI 228) and the westward current increasing since 1998 in the south at mooring AWI 232 (Fig. 3). At mooring AWI 229 north of Maud Rise inter-annual fluctuations dominate.

After averaging the temperature and salinity time series of the water masses (Fig. 5) to the same periods as the geopotential anomaly (Fig. 9), the variations of the flow field and the water mass properties show the clearest correspondence of the decadal fluctuation of the southern limb. The sequence of strong to weak and again strong flow corresponds to cold, warm and again cold temperatures of the WDW, respectively (Table 1). This suggests that a period of strong flow induced a subsequent warm period during which the flow already weakened with a subsequent cooling. The increase in temperature during the second period of strong westward flow is only visible in 2008. The decreasing eastward flow of the northern limb corresponds to increasing temperature and salinity in the WSDW and WSBW.

Under geostrophic conditions, changes of the gyre flow would lead to local or regional temperature and salinity changes, which compensate each other, but not to a net change of the heat content—e.g., stronger flow than average causes cooling in the center of the dome and warming at the periphery and vice versa (Meredith et al., 2008). This must be distinguished from net warming due to regional inflow from outside the gyre related to a net heat gain.

4.3. Ocean–atmosphere interactions

The large-scale circulation of the Weddell gyre is known to be wind-driven (Gordon et al., 1981), while the baroclinic currents are relatively small (Klatt et al., 2005; Whitworth and Nowlin, 1987). This supports the notion that momentum flux by wind stress is readily transferred into the ocean (e.g., Webb and de Cuevas, 2007); hence variation of the wind speed is the prime candidate to explain variability within the gyre. Martinson and Iannuzzi (2003) suggested that there are teleconnections between El Niño–Southern Oscillation and the Weddell gyre flow, as did Gordon et al. (2010) who also found a correlation between the WSBW and the wind variability over the gyre. Jullion et al. (2010) and Meredith et al. (2011) suggest correlations between wind forcing and AABW warming and outflow from the western Weddell gyre.

Since air pressure is the atmospheric property best represented in the ECMWF reanalysis (Uppala et al., 2005), we apply the meridional surface air pressure gradient as a measure for the zonal wind velocity. The low pressure system over the Weddell gyre is centered at 65°S, and thus there is westerly wind north of that latitude and easterly wind south of it (Fig. 10). Consequently, the northern portion of in the southern limb of the gyre with westward flow is usually against the wind, and the southern portion with the wind—in this respect, note that the divide between east and westward water flow, i.e., the axis of the water gyre, is at about 60°S, that is 500 km north of the center of the atmospheric low pressure system (Fig. 10). In accounting for such locally significant features, we calculated time series of air pressure gradients between 60°S and 55°S for the wind belt relevant for the eastward flow in northern limb of the gyre and

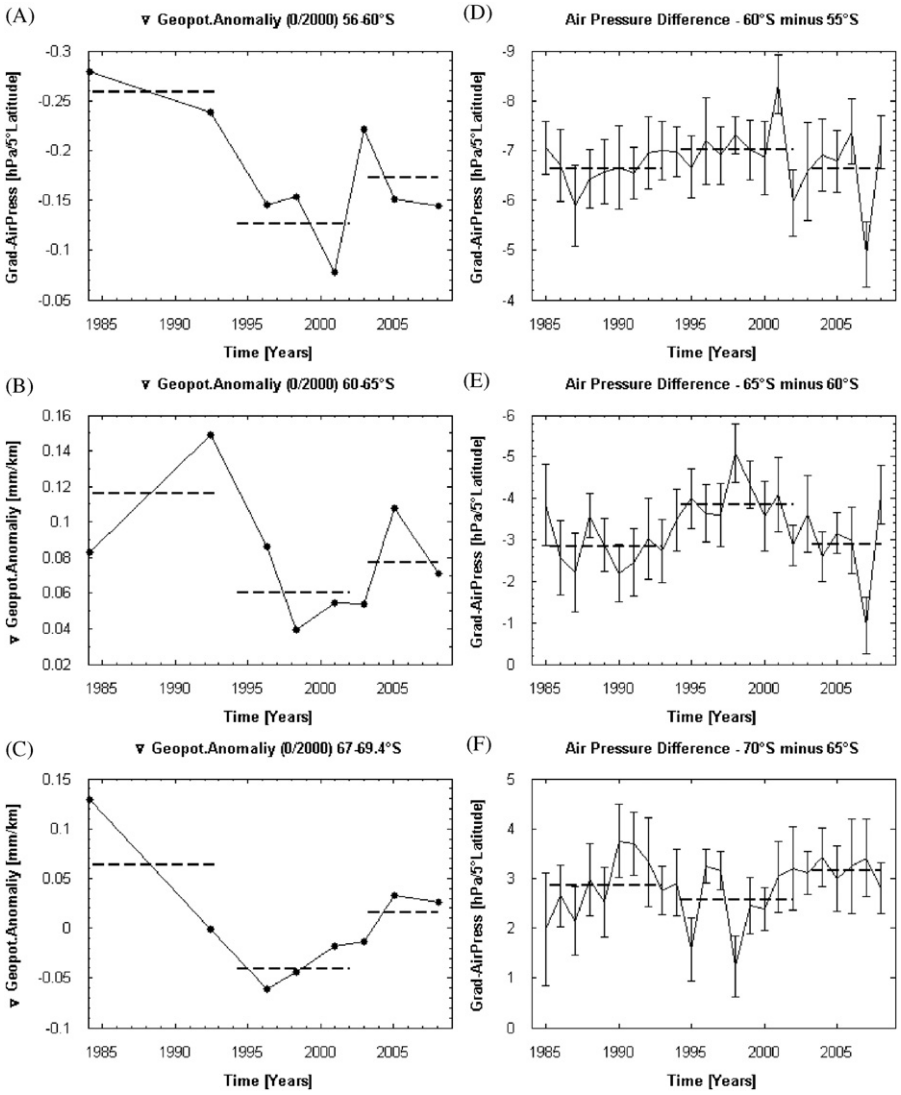

Fig. 9. Time series at the Greenwich meridian of geopotential anomaly gradient (A) in the northern limb of the gyre, (B) in the southern limb of the gyre north of Maud Rise and (C) in the southern limb of the gyre south of Maud Rise. Time series of annual averages of air pressure differences are representative for the northern limb of the gyre (D), the southern limb north of Maud Rise (E) and the southern limb south of Maud Rise (F). The time series are split into three segments from 1984 to 1993, 1994 to 2002 and 2003 to 2008 for which the mean values are indicated by dashed lines.

Table 1
Summary of conditions leading to the three periods of in- or outflow. We distinguish strong and weak flow of the Weddell gyre by the slope of the geopotential anomaly in the northern, central and southern parts, the winds related to air pressure differences, the properties of the water masses (WDW, WSDW and WSBW) and the potential of in- or outflow from the gyre or recirculation within the gyre from the normalized difference and intensity of the eastward and westward gyre flow.

	1984–1993	1993–2003	2003–2008
Slope north	High	Low	Average
Winds north	Low	High	Low
Slope center	High	Low	Average
Wind center	Low	High	Low
Slope south	High	Low	High
Winds south	High	Low	High
WDW	Cold	Warm	Cold
WSDW	Cold	Cold	Warm
WSBW	Cold	Cold	Warm
Inflow/outflow	++	−	+
Recirculation	++	−	+

between 65°S and 60°S for the northern part of the westward water flow and between 70°S and 65°S for the southern portion of it (Fig. 9D–F). It must be admitted that the uncertainties in these time series are relatively large due to large variability of the wind system and the long time intervals from section to section; thus our interpretation cannot claim to be statistically significant. However, we think that by restricting our discussion to the variations of the averages of the three time periods 1984–1993, 1994–2002 and 2003–2008 as we did for the water mass properties and the flow intensity, the observed patterns are robust.

The time series of the air pressure (Fig. 9D–F) depict a consistent structure related to a meridional displacement of the west wind drift during the middle time period of our observations from 1994 to 2002. At the beginning of the time series in the mid-1980s strong westerly winds in the north and weak easterly winds in the south were related to a rather southerly position of the low pressure system, inducing strong eastward flow in the northern Weddell gyre and weak westward flow in the south. In the early 1990s easterly winds increased in the south. In the

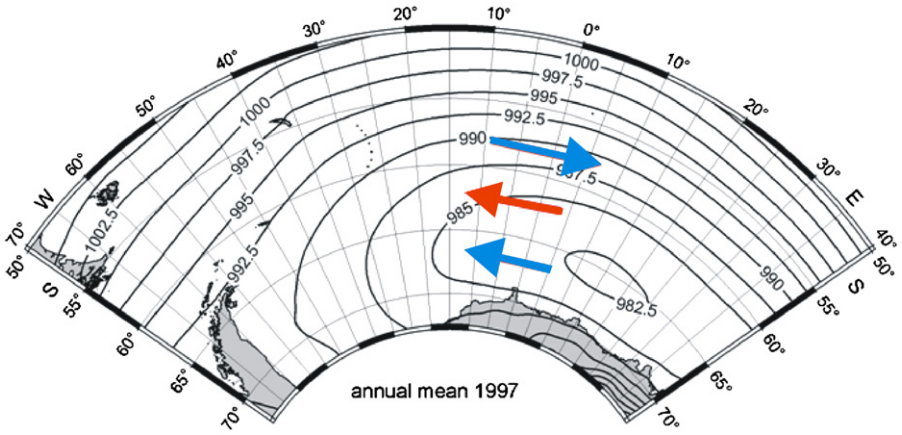

Fig. 10. Surface air pressure in the Atlantic sector of the Southern Ocean from ECMWF data for a typical year, 1997. Arrows indicate the generalized water flow in the northern (to the right) and southern (to the left) limbs of the gyre. The red arrow denotes water that flows against the direction of the prevailing winds. (For interpretation of the references to color in this figure legend, the reader is referred to the web version of this article.)

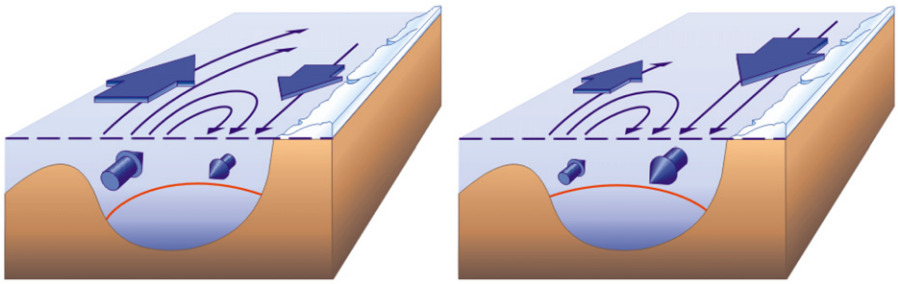

Fig. 11. Schematic representation of the wind system and the Weddell gyre east of the Greenwich meridian. On the left, the situation with strong westerly winds and strong flow in the northern limb of the gyre is displayed; on the right side the inverse situation with weak flow in the north and strong flow in the south with resulting inflow from the east. The shape of the isopycnal surfaces is schematically indicated by a red line. A strong inclination is related to steep dynamic topography and strong flow. (For interpretation of the references to color in this figure legend, the reader is referred to the web version of this article.)

mid- to late-1990s this situation was reversed with strong westerly winds in the north and weak easterly winds in the south. Another reversal back to the previous state occurred in the mid-2000s.

Averaged over the three phases, we can identify corresponding patterns in the wind and in the currents variations (Table 1). Whereas in the northern limb the westerlies show relatively small variations, in the southern limb decadal fluctuations in the order of the mean value dominate. North of Maud Rise weaker westerlies from 1984 to 1993 are followed by stronger westerlies from 1994 to 2002 and weakening again from 2003 to 2008. South of Maud Rise stronger easterlies prevail from 1984 to 1993; they relax from 1993 to 2002 and recover again from 2003 to 2008.

The southern gyre water flow followed this pattern with strong westward flow when the easterly winds were strong and weak westward flow with weak easterly winds (Table 1). The variations of the westerly winds do not affect the flow in the northern and southern limbs of the gyre in a correlated manner, but increasing westerlies enhance the eastward flow in the north and weaken the westward flow in the south. In consequence both limbs of the gyre are not in phase and their water transports differ. Since the gyre is with respect to water masses (except for the Weddell Sea Bottom Water) not bounded by topography in the east and north, strong westward flow in the southern limb is not inconsistent with weak eastward flow in the northern limb or vice versa (Fig. 11). Diverging transports might be compensated by enhanced inflow in the slope current and elevated outflow along the northern boundary of the Weddell gyre, west of the Greenwich meridian (Naveira Garabato et al., 2002b).

We estimated the inflow/outflow conditions by comparing the normalized northern and southern slopes by assuming that on average over the observation period they are balancing each other (Table 1). It turns out that during the first phase from 1984 to 1993 the eastward water flow in the southern part of the gyre was stronger than the flow in the north, resulting in an inflow situation. In the second phase from 1994 to 2002 the northern flow was stronger generating an outflow situation. In the third phase from 2003 to 2008, the northern and southern flows were balanced.

As to the WSBW, it cannot leave the gyre due to the height of the ridges—note, though, that Gordon et al. (2001) suggests that some low-salinity, more oxygenated variety of WSBW, which is recently formed, may leave the gyre in the west. WSBW is transported to the east in the northern gyre flow. We hypothesize that, as in the above case, when there is stronger transport to the west in the southern limb than to the east in the northern gyre limb, a temporal accumulation of WSBW in the west may occur and the amount of WSBW in the eastern part of the gyre would be diminished as during the phase from 1984 to 1993 (Table 1). A comparable result can be obtained when the gyre weakens completely and in consequence the supply of WSBW to the eastern part of the gyre would be slowed down as during the phase from 1994 to 2002. Our data suggests that such a mechanism is active and explains that the area occupied by the WSBW along the section (in the eastern gyre region) decreased significantly from 1992 to 2008 (Fig. 4).

5. Conclusions

Pronounced variations on a multi-annual time scale occurred in the properties of all water masses on the Greenwich meridian

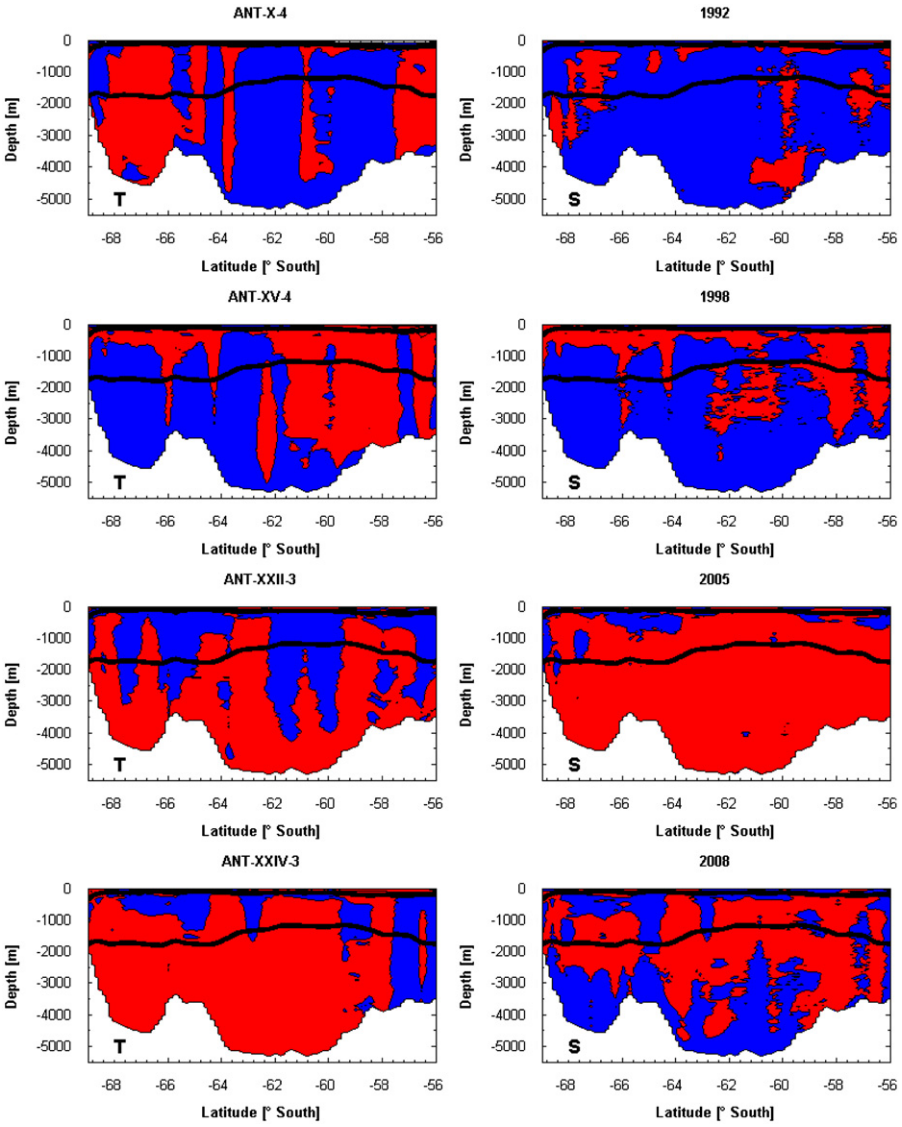

Fig. 12. Difference of potential temperature (left) and salinity (right) of selected sections from 1992 (ANT-X/4), 1998 (ANT-XV/4), 2005 (ANT-XXII/3) and 2008 (ANT-XXIV/3) against the long term means of all sections between 1984 and 2008. Red represents higher temperature and salinity, and blue means lower temperatures and salinity. The black line in the sections represents the lower boundary of the Warm Deep Water. (For interpretation of the references to color in this figure legend, the reader is referred to the web version of this article.)

over a time period of 24 years. The mean WDW temperature increased until the mid-1990s and decreased until 2005. A connection between WDW trends in the Weddell Sea and the adjacent, downstream Scotia Sea may exist (Jullion et al., 2010; Meredith et al., 2008). The mean temperature of the WSDW and the WSBW on the Greenwich meridian has generally risen from the 1980s till 2008.

The long-term changes of the water mass properties are related to changes in the atmospheric driving forces, as displayed by meridional air pressure differences on the Greenwich meridian. In the southern limb of the Weddell gyre with westward water flow, there are periods of far southward reaching westerly winds (thus counteracting water flow) and periods when the easterly winds reach farther to the north (thus less counteracting water flow). According to the variations of geopotential anomaly, which are consistent with current meter records, the northern and the southern limbs of the Weddell gyre vary relatively independently of each other as a consequence of regional wind variations. Strong flow in the north and weak flow in the south implies that not all water from the northern limb can be transferred into the southern limb and in consequence has to abandon the gyre, i.e., in that case the Weddell system supplies more WSDW to the world ocean. For a schematic representation of this situation, see Fig. 11. During periods of stronger westward flow in the south than eastward flow in the north, the flow in the southern limb of the gyre needs replenishing by new inflow into the gyre. This implicates the gyre is open to the east allowing for inflow or outflow of water masses in the gyre area according to the mismatch of westerly and easterly winds. The complicated interaction between water flow and atmospheric forcing of the southern gyre limb combined with the open gyre conditions are the ultimate cause of the fact that southward shifting westerly winds do not necessary lead to gyre flow intensification.

Variations in the northern and southern regimes can be discerned in the inclination of geopotential anomaly. In case of weaker eastward flow in the north, the inclination of the deep isopycnals would decrease, bringing colder WSDW into the depth of the crest of the mid-ocean ridges, which will allow for an easier exit of WSDW from the gyre into ACC and world oceans. Meredith et al. (2008) described such a mechanism to explain variations of

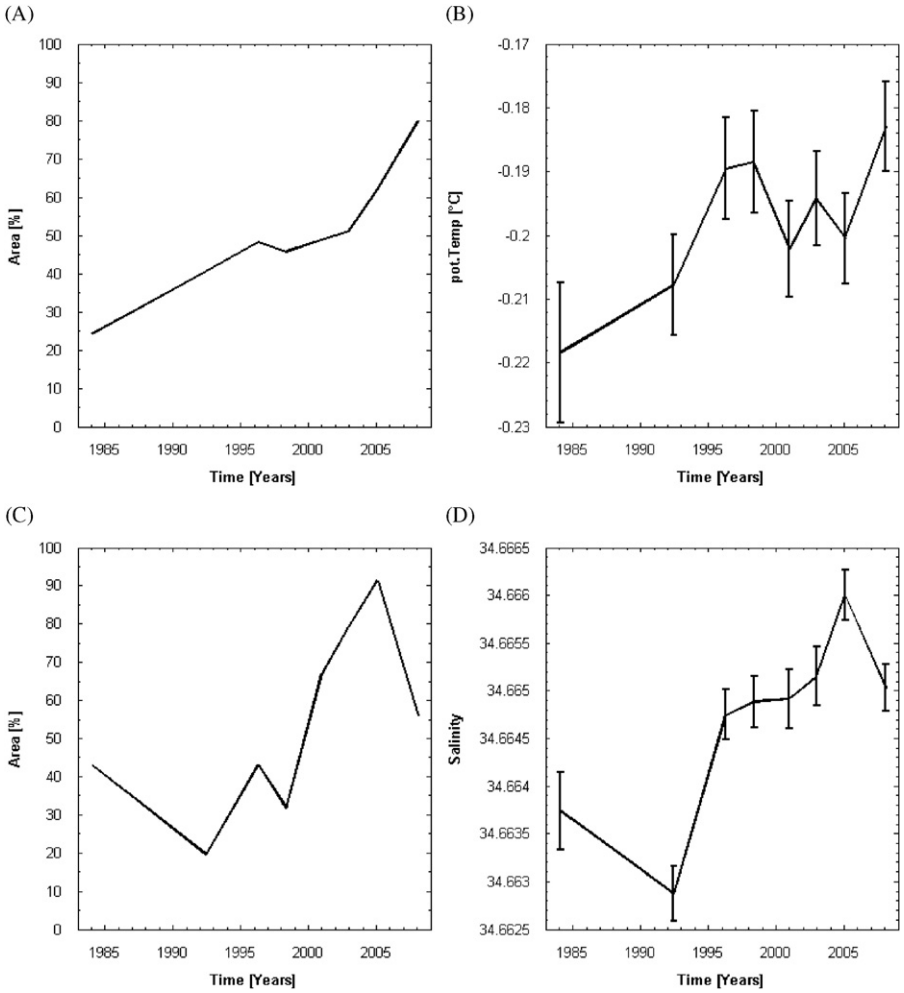

Fig. 13. Time series of the areal extent of temperatures (A) and salinities (C) higher than the long-term average for the section along the Greenwich meridian from 1984 to 2008, and of the potential temperature (B) and salinity (D) averaged over the entire section below 170 m depth.

the WSDW, originating from the Weddell Sea, in the adjacent Scotia Sea. However, stronger flow in the north would also imply stronger WSDW outflow to the east into the Indian Ocean. As a consequence of strong westerly winds in the early 1980s and late 1990s in the area (Fig. 9), we suppose more WSDW to have left the Weddell Sea during these periods.

The circulation of Weddell Sea Bottom Water in the Weddell gyre is controlled by the same ocean–atmosphere processes. Our observations showed that the layer of WSBW found at the Greenwich meridian decreased by 25% in areal extent in 16 years (Fig. 4). The area decrease is spatially biased towards the south, indicating that the warming or loss of cold water has been the strongest there. This is consistent with the stronger flow to the west in the southern limb of the gyre compared with the supply in the north. The corollary to this is that the apparent bottom water warming on the Greenwich meridian need not be caused by reduced formation of WSBW or formation of warmer WSBW in the western Weddell Sea, but that there may be a transient change in the budget of the reservoir in the eastern part of the basin.

One of the outstanding questions is how the Weddell system copes with the changes of the atmospheric driving forces related to climate change. Fyfe (2006) indeed suggests that the temperature trends in the CDW of the Southern Ocean are of anthropogenic nature. A southward shift of the west wind belt has occurred related to a trend to a more positive phase of the Southern Annular Mode before the start of our time series in the early 1980s (Marshall, 2003; Sallée et al., 2010). In the Weddell system the increased and southward displaced westerly winds have been slowing down the southern limb of the gyre. After northward retreat of the westerly winds and increase of the easterly winds in the south in the late 1980s/early 1990s, a warm event was able to penetrate through the gyre. This was terminated by another southward shift of the westerly winds in the mid-1990s followed by the next event in the 2000s leading to new warming. In spite of the sequential inflow events, the area of the section that is warmer than the long term average increased steadily (Fig. 12) from 45% in 1996 to 80% in 2008 (Fig. 13A), consistent with a steady increase of the mean potential temperature of the area between 170 m (excluding the strong seasonal effects of the near surface layer) and the bottom by 0.04 °C (Fig. 13B). Consistent with the potential temperature, the area of salinities above the long-term average (Fig. 13C) and the mean salinity (Fig. 13D) were increasing as well. The effect of the warm pulses appears to have accumulated and transferred the heat into deeper layers. This renders the Weddell system a conduit to bring atmospheric heat into the deep ocean and contribute significantly to the ocean's role as a heat buffer, consistent with Heywood and Stevens (2007). If the heat would have stayed in the 170 m thick near-surface layer and not have been transferred into the deep ocean, this layer would have warmed by about 1 °C over 24 years.

It is worthwhile noting that the new CDW is not being vertically mixed into the deep ocean in the time scales of months

to years. The changes in the deep layers are mainly due to the dynamic effect where stronger flow in the gyre is related to stronger doming. Increase in doming is related to increasing convergence in the dome with warmer and more saline water moving towards the center of the gyre. This lateral shift results in a temperature and salinity increase in the full water column. Only at the boundaries warm water from the CDW can penetrate to greater depths. The same mechanism holds for eddies with a barotropic component, which give rise to correlating changes in the complete water column.

During periods of stronger easterly winds in the early 1990s and 2000s, stronger onshore Ekman transport will have induced stronger downwelling along the continental slope in the south. Simultaneously, stronger westward flow hit the rough topography of Maud Rise most likely increasing mixing there. The Weddell system is not only a prominent contributor to a cool abyssal ocean by way of bottom water formation, which has long been a well known fact. Importantly, it also contributes to a longer-term vertical heat transport due to the formation of warmer and saltier than normal WSDW, which spills into the global ocean thereby serving as a heat buffer to damp global warming for the abyssal oceans.

Acknowledgments

This work is based on seven cruises of FS *Polarstern*. We are grateful to the masters and crews for their ongoing and most dedicated support. We are not able to cite all those by name who contributed by their continuous efforts on land to keep *Polarstern* in operation. We want to thank the reviewers who provided us a great deal of very helpful suggestions. In particular they pushed us towards using neutral density surfaces as water mass boundaries, which increased clearly the visibility of some of the patterns we discuss. We are grateful to the Helmholtz-Gemeinschaft Deutscher Forschungszentren for supporting this research during the MARCOPOLI and PACES programs and to the Bundesministerium für Bildung und Forschung and its predecessors during the WOCE and the CLIVAR projects for maintaining by providing ongoing support the long time series in the Weddell gyre.

References

Andrié, C., Gouriou, Y., Bourlès, B., Termon, J.-F., Braga, E.S., Morin, P., Oudot, C., 2003. Variability of AABW properties in the equatorial channel at 35°W. Geophys. Res. Lett. 30, 8007. doi:10.1029/2002GL015766.

Aoki, S., Rintoul, S.R., Ushio, S., Watanabe, S., Bindoff, N.L., 2005. Freshening of the Adélie Land Bottom Water near 140°E. Geophys. Res. Lett. 32, L23601. doi:10.1029/2005GL024246.

Bagriantsev, N.V., Gordon, A.L., Huber, B.A., 1989. Weddell Gyre: temperature maximum stratum. J. Geophys. Res. 94, 8331–8334.

Böning, C.W., Dispert, A., Visbeck, M., Rintoul, S.R., Schwarzkopf, F.U., 2008. The response of the Antarctic Circumpolar Current to recent climate change. Nat. Geosci 1, 864–869.

Carmack, E.C., 1977. Water characteristics of the Southern Ocean south of the Polar Front. In: Angel, M. (Ed.), A Voyage of Discovery, George Deacon 70th Anniversary Volume. Pergamon Press, Oxford, pp. 15–41.

Carmack, E.C., Foster, T.D., 1975. On the flow of water out of the Weddell Sea. Deep-Sea Res. 22, 711–724.

Chipman, D.W., Takahashi, T., Sutherland, S.C., 1986. Carbon Chemistry of the South Atlantic Ocean and the Weddell Sea: The Results of the Atlantic Long Lines (AJAX) Expeditions, October, 1983–February, 1985. Lamont Doherty Geological Observatory, Palisades, N.Y. 185pp..

Cisewski, B., Strass, V.H., Leach, H., 2011. Circulation and transport of water masses in the Lazarev Sea, Antarctica, during summer and winter 2006. Deep-Sea Res. I 58, 186–199.

Culkin, F., Ridout, P.S., 1998. Stability of IAPSO standard seawater. J. Atmos. Ocean. Technol 15, 1072–1075.

Deacon, G.E.R., 1979. The Weddell Gyre. Deep-Sea Res 26A, 981–995.

Dewey, R.K., 1999. Mooring Design & Dynamics—a Matlab® package for designing and analyzing oceanographic moorings. Mar. Models 1, 103–157.

Dewey, R.K., 2009. Mooring design and dynamics. 〈http://www.mathworks.de/matlabcentral/fileexchange/1629-mooring-design-and-dynamics〉.

Fahrbach, E., De Baar, H. (Eds.), 2010. The Expedition of the Research Vessel "Polarstern" to the Antarctic in 2008 (ANT-XXIV/3). Berichte zur Polar- und Meeresforschung, Vol. 606. Alfred-Wegener-Institut, Bremerhaven 228pp..

Fahrbach, E., Hoppema, M., Rohardt, G., Schröder, M., Wisotzki, A., 2004. Decadal-scale variations of water mass properties in the deep Weddell Sea. Ocean Dyn. 54, 77–91.

Fahrbach, E., Hoppema, M., Rohardt, G., Schröder, M., Wisotzki, A., 2006. Causes of deep-water variation: comment on the paper by L.H. Smedsrud "Warming of the deep water in the Weddell Sea along the Greenwich meridian: 1977–2001". Deep-Sea Res. I 53, 574–577.

Fahrbach, E., Rohardt, G., Scheele, N., Schröder, M., Strass, V., Wisotzki, A., 1995. Formation and discharge of deep and bottom water in the northwestern Weddell Sea. J. Mar. Res. 53, 515–538.

Fahrbach, E., Rohardt, G., Schröder, M., Strass, V., 1994. Transport and structure of the Weddell Gyre. Ann. Geophys. 12, 840–855.

Fahrbach, E., Rohardt, G., Sieger, R., 2007. 25 Years of Polarstern hydrography (1982–2007). WDC-MARE Reports 5, Alfred-Wegener-Institut, Bremerhaven, 94pp.

Foldvik, A., Gammelsrød, T., Østerhus, S., Fahrbach, E., Rohardt, G., Schröder, M., Nicholls, K.W., Padman, L., Woodgate, R.A., 2004. Ice shelf water overflow and bottom water formation in the southern Weddell Sea. J. Geophys. Res. 109, C02015. doi:10.1029/2003JC002008.

Foster, T.D., Carmack, E.C., 1976. Frontal zone mixing and Antarctic Bottom Water formation in the southern Weddell Sea. Deep-Sea Res. 23, 301–317.

Foster, T.D., Foldvik, A., Middleton, J.H., 1987. Mixing and bottom water formation in the shelf break region of the southern Weddell Sea. Deep-Sea Res 34A, 1771–1794.

Fyfe, J.C., 2006. Southern Ocean warming due to human influence. Geophys. Res. Lett. 33, L19701. doi:10.1029/2006GL027247.

Gill, A.E., 1973. Circulation and bottom water production in the Weddell Sea. Deep-Sea Res. 20, 111–140.

Gille, S.T., 2002. Warming of the Southern Ocean since the 1950s. Science 295, 1275–1277.

Gille, S.T., 2008. Decadal-scale temperature trends in the southern hemisphere ocean. J. Climate 21, 4749–4765.

Gordon, A.L., 1982. Weddell Deep Water variability. J. Mar. Res. 40 (Suppl.), 199–217.

Gordon, A.L., Huber, B., McKee, D., Visbeck, M., 2010. A seasonal cycle in the export of bottom water from the Weddell Sea. Nat. Geosci. 3, 551–556.

Gordon, A.L., Martinson, D.G., Taylor, H.W., 1981. The wind-driven circulation in the Weddell–Enderby basin. Deep-Sea Res 28A, 151–163.

Gordon, A.L., Visbeck, M., Huber, B., 2001. Export of Weddell Sea Deep and Bottom Water. J. Geophys. Res. 106, 9005–9017.

Gouretski, V.V., Danilov, A.I., 1993. Weddell Gyre: structure of the eastern boundary. Deep-Sea Res. I 40, 561–582.

Gouretski, V., Koltermann, K.P., 2007. How much is the ocean really warming? Geophys. Res. Lett. 34, L01610. doi:10.1029/2006GL027834.

Hall, A., Visbeck, M., 2002. Synchronous variability in the southern hemisphere atmosphere, sea ice, and ocean resulting from the annular mode. J. Climate 15, 3043–3057.

Heywood, K.J., Sparrow, M.D., Brown, J., Dickson, R.R., 1999. Frontal structure and Antarctic Bottom Water flow through the Princess Elizabeth Trough, Antarctica. Deep-Sea Res. I 46, 1181–1200.

Heywood, K.J., Stevens, D.P., 2007. Meridional heat transport across the Antarctic Circumpolar Current by the Antarctic Bottom Water overturning cell. Geophys. Res. Lett. 34, L11610. doi:10.1029/2007GL030130.

Hoppema, M., Klatt, O., Roether, W., Fahrbach, E., Bulsiewicz, K., Rodehacke, C., Rohardt, G., 2001. Prominent renewal of Weddell Sea Deep Water from a remote source. J. Mar. Res. 59, 257–279.

Jackett, D.R., McDougall, T.J., 1997. A neutral density variable for the world's oceans. J. Phys. Oceanogr. 27, 237–263.

Johnson, G.C., Purkey, S.G., Bullister, J.L., 2008. Warming and freshening in the abyssal Southeastern Indian Ocean. J. Climate 21, 5351–5363.

Jullion, L., Jones, S.C., Naveira Garabato, A.C., Meredith, M.P., 2010. Wind-controlled export of Antarctic Bottom Water from the Weddell Sea. Geophys. Res. Lett. 37, L09609. doi:10.1029/2010GL042822.

Kerr, R., Mata, M.M., Garcia, C.A.E., 2009. On the temporal variability of the Weddell Sea deep water masses. Antarctic Sci. 21, 383–400.

Klatt, O., Boebel, O., Fahrbach, E., 2007. A profiling float's sense of ice. J. Atmos. Oceanic Technol 24, 1301–1308.

Klatt, O., Fahrbach, E., Hoppema, M., Rohardt, G., 2005. The transport of the Weddell Gyre across the Prime Meridian. Deep-Sea Res. II 52, 513–528.

Leach, H., Strass, V., Cisewski, B., 2011. Modification by lateral mixing of the Warm Deep Water entering the Weddell Sea in the Maud Rise region. Ocean Dyn. 61, 51–68.

Levitus, S., Antonov, J., Boyer, T., 2005. Warming of the world ocean, 1955–2003. Geophys. Res. Lett. 32, L02604. doi:10.1029/2004GL021592.

Lindsay, R.W., Kwok, R., De Steur, L., Meier, W., 2008. Halo of ice deformation observed over the Maud Rise seamount. Geophys. Res. Lett. 35, L15501. doi:10.1029/2008GL034629.

Marshall, G.J., 2003. Trends in the Southern Annular Mode from observations and reanalyses. J. Climate 16, 4134–4143.

Martinson, D.G., Iannuzzi, R.A., 2003. Spatial/temporal patterns in Weddell gyre characteristics and their relationship to global climate. J. Geophys. Res., 108. doi:10.1029/2000JC000538.

McDougall, T.J., Jackett, D.R., 2004. The material derivative of neutral density. J. Mar. Res. 63, 159–185.
Meredith, M.P., Gordon, A.L., Naveira Garabato, A.C., Abrahamsen, E.P., Huber, B.A., Jullion, L., Venables, H.J., 2011. Synchronous intensification and warming of Antarctic Bottom Water outflow from the Weddell Gyre. Geophys. Res. Lett. 38, L03603. doi:10.1029/2010GL046265.
Meredith, M.P., Locarnini, R.A., Van Scoy, K.A., Watson, A.J., Heywood, K.J., King, B.A., 2000. On the sources of Weddell Gyre Antarctic Bottom Water. J. Geophys. Res. 105, 1093–1104.
Meredith, M.P., Naveira Garabato, A.C., Gordon, A.L., Johnson, G.C., 2008. Evolution of the deep and bottom waters of the Scotia Sea, Southern Ocean, during 1995–2005. J. Climate 21, 3327–3343.
Meredith, M.P., Naveira Garabato, A.C., Stevens, D.P., Heywood, K.J., Sanders, R.J., 2001. Deep and bottom waters in the eastern Scotia Sea: rapid changes in properties and circulation. J. Phys. Oceanogr. 31, 2157–2168.
Mosby, H., 1934. The waters of the Atlantic Antarctic Ocean. Scientific Results of the Norwegian Antarctic Expeditions 1927-1928 1 (11), 1–131.
Muench, R.D., Morison, J.H., Padman, L., Martinson, D., Schlosser, P., Huber, B., Hohmann, R., 2001. Maud Rise revisited. J. Geophys. Res. 106, 2423–2440.
Naveira Garabato, A.C., Heywood, K.J., Stevens, D.P., 2002a. Modification and pathways of Southern Ocean Deep Waters in the Scotia Sea. Deep-Sea Res. I 49, 681–705.
Naveira Garabato, A.C., McDonagh, E.L., Stevens, D.P., Heywood, K.J., Sanders, R.J., 2002b. On the export of Antarctic Bottom Water from the Weddell Sea. Deep-Sea Res. II 49, 4715–4742.
Nicholls, K.W., Østerhus, S., Makinson, K., Gammelsrød, T., Fahrbach, E., 2009. Ice-ocean processes over the continental shelf of the southern Weddell Sea, Antarctica: a review. Rev. Geophys. 47, RG3003. doi:10.1029/2007RG000250.
Núñez-Riboni, I., Fahrbach, E., 2009. Seasonal variability of the Antarctic Coastal Current and its driving mechanisms in the Weddell Sea. Deep-Sea Res. I 56, 1927–1941.
Orsi, A.H., Johnson, G.C., Bullister, J.L., 1999. Circulation, mixing, and production of Antarctic Bottom Water. Progr. Oceanogr 43, 55–109.
Orsi, A.H., Nowlin Jr., W.D., Whitworth III, T., 1993. On the circulation and stratification of the Weddell Gyre. Deep-Sea Res. I 40, 169–203.
Owens, W.B., Wong, A.P.S., 2009. An improved calibration method for the drift of the conductivity sensor on autonomous CTD profiling floats by θ–S climatology. Deep-Sea Res. I 56, 450–457.
Purkey, S.G., Johnson, G.C., 2010. Warming of global abyssal and deep Southern Ocean waters between the 1990s and 2000s: contributions to global heat and sea level rise budgets. J. Climate 23, 6336–6351.
Reid, J.L., Nowlin Jr., W.D., Patzert, W.C., 1977. On the characteristics and circulation of the southwestern Atlantic Ocean. J. Phys. Oceanogr. 7, 62–91.
Rintoul, S.R., 1998. On the origin and influence of Adélie Land Bottom Water. In: Jacobs, S.S., Weiss, R.F. (Eds.), Ocean, Ice, and Atmosphere: Interactions at the Antarctic Continental Margin. Antarctic Research Series 75. American Geophysical Union, Washington, D.C, pp. 151–171.
Rintoul, S.R., 2007. Rapid freshening of Antarctic Bottom Water formed in the Indian and Pacific Oceans. Geophys. Res. Lett. 34, L06606. doi:10.1029/2006GL028550.
Rintoul, S.R., Hughes, C.W., Olbers, D., 2001. The Antarctic Circumpolar Current system. In: Siedler, G., Church, J., Gould, J. (Eds.), Ocean Circulation and Climate: Observing and Modelling the Global Ocean. Academic Press, London, pp. 271–302.
Robertson, R., Visbeck, M., Gordon, A.L., Fahrbach, E., 2002. Long-term temperature trends in the deep waters of the Weddell Sea. Deep-Sea Res. II 49, 4791–4806.
Sallée, J.B., Speer, K.G., Rintoul, S.R., 2010. Zonally asymmetric response of the Southern Ocean mixed-layer depth to the Southern Annular Mode. Nat. Geosci. 3, 273–279.
Schlitzer, R., 2010. Ocean Data View 〈http://odv.awi.de〉.
Schlosser, P., Bullister, J.L., Bayer, R., 1991. Studies of deep water formation and circulation in the Weddel Sea using natural and anthropogenic tracers. Mar. Chem 35, 97–122.
Schmitz Jr., W.J., 1996. On the world ocean circulation: volume II, The Pacific and Indian Oceans/a global update. Woods Hole Oceanographic Institution, Technical Report, WHOI 96-08, 237pp.
Schröder, M., Fahrbach, E., 1999. On the structure and the transport of the eastern Weddell Gyre. Deep-Sea Res. II 46, 501–527.
Siedler, G., Church, J., Gould, J. (Eds.), 2001. Ocean Circulation and Climate: Observing and Modelling the Global Ocean. Academic Press, London.
Smedsrud, L.H., 2005. Warming of the deep water in the Weddell Sea along the Greenwich meridian: 1977–2001. Deep-Sea Res. I 52, 241–258.
Sprintall, J., 2008. Long-term trends and interannual variability of temperature in Drake Passage. Progr. Oceanogr 77, 316–330.
Thompson, D.W.J., Solomon, S., 2002. Interpretation of recent Southern Hemisphere climate change. Science 296, 895–899.
Uppala, S.M., Kållberg, P.W., Simmons, A.J., Andrae, U., da Costa Bechtold, V., Fiorino, M., Gibson, J.K., Haseler, J., Hernandez, A., Kelly, G.A., Li, X., Onogi, K., Saarinen, S., Sokka, N., Allan, R.P., Andersson, E., Arpe, K., Balmaseda, M.A., Beljaars, A.C.M., Van de Berg, L., Bidlot, J., Bormann, N., Caires, S., Chevallier, F., Dethof, A., Dragosavac, M., Fisher, M., Fuentes, M., Hagemann, S., Hólm, E., Hoskins, B.J., Isaksen, L., Janssen, P.A.E.M., Jenne, R., McNally, A.P., Mahfouf, J.-F., Morcrette, J.-J., Rayner, N.A., Saunders, R.W., Simon, P., Sterl, A., Trenberth, K.E., Untch, A., Vasiljevic, D., Viterbo, P., Woollen, J., 2005. The ERA-40 re-analysis. Quart. J.R. Meteorol. Soc. 131, 2961–3012.
Webb, D.J., de Cuevas, B.A., 2007. On the fast response of the Southern Ocean to changes in the zonal wind. Ocean Sci 3, 417–427.
Weppernig, R., Schlosser, P., Khatiwala, S., Fairbanks, R.G., 1996. Isotope data from Ice Station Weddell: implications for deep water formation in the Weddell Sea. J. Geophys. Res. 101, 25723–25739.
Whitworth III, T., Nowlin Jr., W.D., 1987. Water masses and currents of the Southern Ocean at the Greenwich meridian. J. Geophys. Res. 92, 6462–6476.
Zenk, W., Morozov, E., 2007. Decadal warming of the coldest Antarctic Bottom Water flow through the Vema Channel. Geophys. Res. Lett. 34, L14607. doi:10.1029/2007GL030340.